Sensitivity of climate change detection and attribution to the characterization of internal climate variability

Jara Imbers

OCCAM, Mathematical institute, University of Oxford

Ana Lopez

Center for the Analysis of time series, London School of Economics

Chris Huntingford

Centre for Ecology and Hydrology

Myles Allen

Atmospheric, Oceanic and Planetary Physics, University of Oxford

Corresponding author address: Jara Imbers, OCCAM , Mathematical Institute, 24 - 29 St Giles', Oxford, OX1 3LB.

E-mail: imbers@maths.ox.ac.uk

ABSTRACT

1. Introduction

At the centre of the climate change debate is the question of whether global warming can be detected, and if that is the case, whether or not it can be attributed to anthropogenic causes. Optimal fingerprinting is a powerful method of detection and attribution of climate change (Hasselmann 1979, 1993; Hegerl et al. 1996) used widely in this area of research. In essence, optimal fingerprinting is a multi-regression analysis that searches for the observed temperature record response to external drivers or forcings such as changing levels of greenhouse gases, and aerosol loading (human-induced), volcanic activity and variations in solar radiation (naturally induced). A key input in the procedure of fitting this multiple regression model is an estimate of the internal variability of the climate system, against which the statistical significance of anthropogenic and natural signals must be compared. Hence, an accurate depiction of this variability is crucial for the robustness of the results.

In this work we refer to internal variability as the characterization of the variations in the climate system that would occur in the absence of natural or anthropogenic forcings, solely due to the coupling of atmosphere, ocean, biosphere and cryosphere dynamics. In most cases Global Climate Models (GCMs) are used to estimate climate internal variability bilitldbili0d0 g 0tion of w authors are careful to attempt the inclusion of model uncertainty in the regression model, and test the robustness of their results under changes in the amplitude of the estimated internal variability, it is not clear whether or not other aspects of the internal variability

where T is the global mean temperature and F is the external forcing. In Allen et al. (2009), the heat capacity $c = 7.22 \frac{W\,y}{m^2\,K}$ corresponds to the heat capacity of an ocean mixed layer of depth $d_{ml} = 75m$ assuming that the ocean covers 70% of the Earth surface. Best estimates for the climate feedback parameter and e ective fnhJ/F1ctive75 data set to test the sensitivity of the results to the addition of the last seven years of observations up to 2012 (see section 3). Uncertainties in observed temperatures and estimates of forcings are ignored in this paper.

We additionally use the World Climate Research Programme (WCRP) CMIP3 multi-model archive of control simulations to study the internal variability simulated by the state of the art climate models (Solomon 2007). For completeness, we have used all the control simulations, regardless of drifts. We will comment on the effect of drifts in the control segments on the final results in Section 3.

(i) Detection and Attribution

The detection of climate change is the process of demonstrating that climate has changed in some well defined statistical sense, without providing a reason for that change. Attribution of causes of climate change is the process of establishing the most likely causes for the detected change with some defined level of confidence (Solomon 2007). In this work we aim to detect and attribute climate change by estimating the contribution to the observational record T_{obs} of each of the response temperatures T_i calculated using Eq.(1). In other words, we want to obtain the amplitudes β_i in the following expression:

$$T_{obs} = T\beta + u; \tag{2}$$

where T is a matrix with $n + 1$ columns including the n forced responses T_i, and a constant term to remove the mean. u is an stochastic term that represents the internal climate variability with covariance matrix is given by $\Sigma = E(uu^{\dagger})$. Under the assumption that u is multivariate normal (Allen and Tett 1999), the optimal scaling factors, $\beta = (\beta_1; \beta_2; \ldots \beta_{n+1})$ are given by (Kmenta 1971):

$$\hat{\beta} = \left(T^{\dagger}\Sigma^{-1}T\right)^{-1}T^{\dagger}\Sigma^{-1}T_{obs}; \tag{3}$$

and their variance :

$$V(\hat{\ }) = \ T^{y} \quad {}^{1}T \quad {}^{1}; \tag{4}$$

where *y* is used to denote the transpose of a matrix.

In this work, following standard detection and attribution studies, we consider the following external forcings: greenhouse gases, sulphates, volcanic and solar. It has long been recognized however, that the detection and attribution results are sensitive to the omission of potentially important forcings and/or internal modes of variability. Likewise, if signals that terize the global mean internal variability u explicitly as a stationary stochastic process. In other words, we formulate the detection and attribution problem as in Eq.(2) but with u a function of stochastic parameters that are estimated simultaneously with the scaling factors ^ using a minimum squared error algorithm.

The first challenge is to choose an adequate stochastic representation for the internal variability. The difficulties finding the appropriate stochastic model are due to the uncertainties in characterizing internal variability from the observational record, which as discussed before, is contaminated by the external forcings and too short relative to the long time scales potentially relevant to the current climate variability . In particular, in the observed record it is not clear how to separate the decadal from centennial or even longer time scales (Percival et al. 2001). Given these uncertainties in the characterization of the internal climate variability we choose to describe it using two models that span a wide range of plausible temporal autocorrelations (Vyushin and Kushner 2009). This choice is important to address the fact between oceanic and atmospheric dynamics. In this framework, the faster dynamics of the atmosphere can be modeled as white noise acting on the slower and damped dynamics of the ocean. Thus, the AR(1) is the simplest model that can explain the \weather " and the \climate" uctuations as two components of the internal variability. Mathematically, the AR(1) is a stationary stochastic process that can be written as:

$$u_t = a_1 u_{t \quad 1} + a_0 \quad_t \tag{5}$$

where $E(u_t) = 0$, a_1 and a_0 are parameters, and $\quad_t$ represents white noise, .e. $E(\quad_t \quad_{t^0}) = \quad_{tt^0}$. The autocovariance function of this process is determined by a_0 and a_1 as follows:

$$!_{AR\,1}(\quad) = \frac{a_0^2}{1 \quad a_1^2} a_1^{j \quad j} \tag{6}$$

where is the time lag. Notice that a_1 controls the decaying rate of the autocorrelation function and in that sense we can associate it to the memory of the system. On the other hand a_0 is related to the amplitude of the white noise in the system. From Eq.(6) the covariance matrix results:

$$^{AR}_{i;j} = \frac{a_0^2}{1 \quad a_1^2} a_1^{ji \quad jj} \tag{7}$$

Eq.(5) models the memory of the process such that at a given time t the state of the system is a linear function of the previous state (t 1) and some random noise with amplitude a_0^2 jittering, and hence moving the system away from equilibrium. The autocovariance of the process, Eq.(6), decays exponentially with time, so the system has always a much better memory of the near past than of the distant past. a_1 can take any value in the interval $[0; 1)$, $a_1 = 0$ represents the limit in which the system is purely white noise, and $a_1 \; ! \; 1$ is the

the parameters a_1 and a_0 of the climate noise in Eq.(5) following the Hildreth-Lu method (Kmenta 1971).

(iii) Long memory process: FD

There is empirical evidence that the spectrum of global mean temperature is more complex than the spectrum of an AR(1) process (e.g. Huybers and Curry (2006)). Different power-law behaviors have been identified in globally and hemispherically averaged surface

$$u_t = (1 - B)^{-d} \epsilon_t. \tag{8}$$

where B is the backshift operator, i.e. $Bu_t = u_{t-1}$ (Beran 1994). The model is fully specified by the parameters d and the standard deviation σ_e of the white noise ϵ_t. The autocovariance function is given by the equation:

$$\omega_{FD}(\tau) = \frac{\sigma_e^2 \sin(\pi d)\,\Gamma(1-2d)\,\Gamma(\tau+d)}{\pi\,\Gamma(\tau+1-d)} \tag{9}$$

As a result the covariance matrix becomes,

$$\Sigma_{i,j}^{FD} = \frac{\sigma_e^2 \sin(\pi d)\,\Gamma(1-2d)\,\Gamma(|i-j|+d)}{\pi\,\Gamma(|i-j|+1-d)}. \tag{10}$$

For large τ the autocorrelation function satisfies $\lim_{\tau\to\infty} \omega_{FD}(\tau) = |\tau|^{2d-1}$ (Beran 1994). From this expression one can see that the autocorrelation decays algebraically, thus the name "long memory". Since d controls the decaying rate of the autocorrelation function it can be associated to the memory of the system, while σ_e is characterizes the amplitude of the white noise.

Similarly to the AR(1) case, we use this covariance matrix, Eq.(10), and Eq.(2) and Eq.(3) to simultaneously determine the scaling factors β_i and the parameters d and σ_e following the Hildreth-Lu method (Kmenta 1971).

3. Results

a. Robustness of detection statistics

In order to test the robustness of the detection statistics, we find simultaneously the scaling factors β_i and the stochastic parameters of the internal variability u, using generalized linear regression to solve Eq.(2). Notice that when u is modeled as an AR(1) or an FD process, the noise covariance matrix Σ in Eq.(3) and Eq.(4) is given by Eq.(7) or Eq.(10) respectively. The best estimates of the scaling and noise parameters are chosen as those that minimize the residual white noise in u (Kmenta 1971). Using the Akaike Information Criteria we find that both models for u are equally skilful at representing the internal variability given the observational record used in our analysis.

Fig.(1) shows the values of the optimal scaling factors with their 95% confidence intervals using the AR(1) (grey line) and the FD (black line) models, when T_{obs} is the HadCRUT3 global mean temperature record for the period 1850-2005. In the detection and attribution approach, a signal is detected when the corresponding scaling factor is different from 0 with 95% confidence, while the attribution of a signal requires confidence intervals that include given value of the z_score or, equivalently, the size of the confidence interval, we aim to find what is the proportion of cases where the scaling factor is different from 0. In particular the value of the z_score that gives different from 0 in at most 5% of the cases determines the 95% confidence interval. We find that for the GHG signal the z_score is 2:22 in the case of the AR(1) model and 2:45 in the case of the FD model. In addition, and since we expect that due to the stochastic nature of the noise models there will be some uncertainty in the determination of their parameters, the values of the noise model parameters estimated with this Monte Carlo approach provide an estimate of the uncertainty of the best fit noise model parameters when regressing the forced responses on T_{obs} in Eq.(2).

Fig.(1) shows that for our detection model, the greenhouse gas signal is detected and attributed, the volcanic signal is only detected, and the solar signal is not detected nor attributed for both models of internal variability. In the case of the sulphates forcings, the result depends on the representation of the internal variability.

The robustness of the GHG signal detection can be analyzed using Fig.(2) when the internal variability is characterized by the AR(1) model or by the FD model in the upper or lower panels respectively. The horizontal and vertical axes show the white noise amplitude and memory parameters respectively, and the contour lines indicate the significance level of the scaling factor $_{GHG}$. The diamond symbol shows the best fit of internal variability (for each model) when the observed record T_{obs} is the HADCRUT3 data for the period 1850-2005. The uncertainty in the estimation of the best fit, computed using the Monte Carlo approach, is shown as the grey cloud of points. It is clear that even when taking into account this uncertainty in the parameters, the significance of the detection of the greenhouse gas signal is not affected.

As expected, the significance of the greenhouse gas signal is lower when we represent the internal variability as an FD than as an AR(1) process. We find that both stochastic models' best fit have similar white noise amplitude, showing that statistically they are similarly good at explaining variability, given that this is the residual of the linear fit. The bigger difference between the two models arises in the memory parameter.

In the case of the AR(1), a_1 is bounded between $a_1 = 0{:}25$ and $a_1 = 0{:}70$, and the best estimate is $a_1 = 0{:}$

the time it takes for the autocorrelation function to reduce to $1/e$ of its initial value (in analogy with the e-folding time for the AR(1) model). For the best fit value of $= 0.43$ for instance, this calculation gives a much longer time than the length of the observational record (156 years). This suggests that, according to this model, in the 156 years long record all points are highly correlated. Overall, we find that, despite the very different time scales that are relevant for the AR(1) and FD characterizations of internal variability, the GHG signal detection statistics is robust for both models.

One interesting question that can be explored using our results is how wrong one would have to get the model parameters of the internal variability in order to change the detection statement of the greenhouse gas signal. In the case of the AR(1) model we find that the greenhouse gas signal would become not statistically significant in a world in which higher values of a_1 and/or a_0 were needed to describe internal variability. In the upper panel of Fig.2 we see that, to loose statistical significance, one would have to increase the time correlation characterized by a_1 to more than 0.8 , or triple the white noise parameter a_0.

Hence, the detection statistics for the AR(1) model is very sensitive to the memory parameter and relatively less sensitive to the amount of white noise in the process. Thus, in terms of the global mean temperature internal variability as simulated by GCMs, our findings suggest that the relevant aspect that should be taken into account in a robustness test should be the models' ability to capture correctly the temporal correlations more than the total variance, which is in turn conditioned by their ability to capture the most relevant dynamical processes, their couplings and feedback mechanisms.

For the FD process we find a different result. In the lower panel of Fig.(2) we can see that for the estimated ${}_e$ there is no for which the process has a greenhouse gas scaling factor which is not statistically significant. Thus, this suggests that the greenhouse gases detection results are robust under changes in the memory parameter. In fact, for very high values of

b. CMIP-3 control runs

In this section we use the same techniques as above to evaluate the control simulations used in the detection and attribution of climate change included in the 4th Assessment Report of the IPCC. Our goal is to get some insight about the controls' potential limitations to estimate internal variability and how this might impact in the robustness of the detection and attribution statistics.

We take annual global mean temperature segments from the CMIP3 control simulations that have the same length as the observational record, 156 years, and t them to an AR(1)

equivalent to finding similar covariance matrices; hence this figure is consistent with our previous findings about the similarity in magnitude of the autocorrelation functions of the fitted internal variability to the 156 years observed record. It is clear that a much longer time series is required to appreciate more significant differences in the variability simulated by the two stochastic models.

We can also analyze the link between the ability of a GCM to model different modes of internal variability and the implications for the significance of detection and attribution. It is clear from Fig.(4) that some control segments display peaks corresponding to the ENSO signal with unrealistic high amplitudes , as shown by the high power at the 2-5 years frequency range. However, Fig.(2) shows that most of these control segments fall in the area of the plots that correspond to a significant greenhouse gas signal. Consistently wit the findings in Allen and Tett (1999), this analysis suggests that an accurate depiction of all modes of internal variability might not be required to ensure the robustness of the detection statistics under our detection model.

Finally, our analysis point towards the need to develop a wider range of techniques to assess the robustness of detection and attribution of climate change. The \consistency test" described in Allen and Tett (1999) is equivalent to look at the power spectra of GCMs runs and compare their (typically) decadal internal variability with the decadal internal variability retained in the residuals of the fit to the observed record. The aim of this test is mainly to discard the possibility of over-attributing climate change to the anthropogenic signal only because climate models under-represent decadal variability. However, studying just the amplitude (or power) of internal variability in Fig.(4) does not give us information about all the possible impacts that a model imperfection might have on the detection and attribution statistics. Thus, there is a need to develop techniques that provide a way to evaluate the impact of specific modes of variability and their interactions, and not just their amplitude, on the detection and attribution of climate change. Many interesting studies have been developed recently (eg. DelSole et al. (2011)) but more work is needed. One

models are chosen to span a wide range of plausible temporal autocorrelation structures, and include the short-memory first-order autoregressive (AR(1)) process and the long-memory fractionally differencing (FD) process). We find that, independently of the representation chosen, the greenhouse gas signal remains statistically significant under the detection model

APPENDIX A

We use a HadCM3 control simulation of 1000 years to assess how the uncertainty of the stochastic parameters depends on the length of the segment, and we refer to this as a nite

REFERENCES

Allen, M., D. J. Frame, C. Huntigford, C. D. Jones, J. Lowe, M. Meinshausen, and N. Meinhausend, 2009: Warming caused by cumulative carbon emissions towards the trillionth tonne. Nature, 458, 1163{1166.

Allen, M. and P. Stott, 2003: Estimating signal amplitudes in optimal ngerprinting, part I: Theory. Climate Dynamics, 21 (5), 477{491.

Allen, M. and S. Tett, 1999: Checking for model consistency in optimal ngerprinting. Climate Dynamics, 15 (6), 419{434.

Andrews, D. G. and M. R. Allen, 2008: Diagnosis of climate models in terms of transient climate response and feedback response time. Atmospheric Science Letters, 9 (1), 7{12.

Beran, J., 1994: Statistics for long-memory processes, Vol. 61. Chapman & Hall, New York.

Bloom eld, P., 1992: Trends in global temperature. Climatic Change, 21 (1), 1{16.

Bretherton, C. and D. Battisti, 2000: Interpretation of the results from atmospheric general circulation models forced by the time history of the observed sea surface temperature distribution. Geophysical research letters, 27 (6), 767{770.

Brohan, P. et al., 2006: Uncertainty estimates in regional and global observed temperature changes: A new dataset from 1850. J. Geophys. research, 111, D12 106.

DelSole, T. and J. Shukla, 2010: Model delity versus skill in seasonal forecasting. Journal of Climate, 23 (18), 4794{4806.

DelSole, T., M. Tippett, and J. Shukla, 2011: A signi cant component of unforced multidecadal variability in the recent acceleration of global warming. Journal of Climate, 24 (3), 909{926.

Erland, S., P. Greenwood, and L. Ward, 2011: 1=f noise is equivalent to an eigenstructure power relation. Europhysics Letters, Volume, 95 (6), 60006.

Esper, J., et al., 2012: Orbital forcing of tree-ring data. Nature Climate Change

Ghil, M., 2001: Hilbert problems for the geosciences in the 21st century. Nonlinear Processes in Geophysics, 8 (4/5), 211{211.

Ghil, M., 2012: Climate variability: Nonlinear and random e ects. Encyclopedia of Atmospheric Sciences.

Ghil, M., et al., 2002: Advanced spectral methods for climatic time series. Rev. Geophys, 40 (1), 1003.

Gil-Alana, L., 2005: Statistical modeling of the temperatures in the northern hemi g 0 l 584

Huntingford, C., P. Stott, M. Allen, and F. Lambert, 2006: Incorporating model uncertainty into attribution of observed temperature change. Geophysical Research Letters, 33 (5), L05 710.

Hurst, H., 1951: Long-term storage capacity of reservoirs. Trans. Amer. Soc. Civil Eng., 116, 770{808.

Hurst, H., 1957: A suggested statistical model of some time series which occur in nature. Nature, 180, 494.

Huybers, P. and W. Curry, 2006: Links between annual, Milankovitch and continuum temperature variability. Nature, 441 (7091), 329{332.

Imbers, J., A. Lopez, C. Huntingford, and M. Allen, 2013: Testing the robustness of the anthropogenic climate change detection statements using different empirical models. Journal of Geophysical Research: Atmospheres, 1{8.

Kaulakys, B., J. Ruseckas, V. Gontis, and M. Alaburda, 2006: Nonlinear stochastic models of 1/f noise and power-law distributions. Physica A: Statistical Mechanics and its Applications, 365 (1), 217{221.

Klein, S., B. Soden, and N. Lau, 1999: Remote sea surface temperature variations during enso: Evidence for a tropical atmospheric bridge. Journal of Climate, 12 (4), 917{932.

Kmenta, J., 1971: Elements of econometrics. Macmillan New York.

Levitus, S., J. Antonov, and T. Boyer, 2005: Warming of the world ocean, 1955-2003. Geophys. Res. Lett, 32, L02 604.

Meinshausen, M., et al., 2011: The rcp greenhouse gas concentrations and their extensions from 1765 to 2300. Climatic Change, 109 (1-2), 213{241.

Mitchell, J. et al., 1976: An overview of climatic variability and its causal mechanisms. Quaternary Research, 6 (4), 481{493.

Morice, C. P., J. J. Kennedy, N. A. Rayner, and P. D. Jones, 2012: Quantifying uncertainties in global and regional temperature change using an ensemble of observational estimates: The hadcrut4 data set. Journal of Geophysical Research: Atmospheres (1984{2012), 117 (D8).

Newman, M., P. Sardeshmukh, and C. Penland, 2009: How important is air-sea coupling in enso and mjo evolution? Journal of Climate, 22 (11), 2958{2977.

Pelletier, J., 1997: Analysis and modeling of the natural variability of climate. Journal of climate, 10 (6), 1331{1342.

Percival, D., J. Overland, and H. Mofjeld, 2001: Interpretation of north paci c variability as a short-and long-memory process. Journal of climate, 14 (24), 4545{4559.

Solomon, S., 2007: Climate change 2007: the physical science basis: contribution of Working Group I to the Fourth Assessment Report of the Intergovernmental Panel on Climate Change Cambridge Univ Pr.

Stone, D., M. Allen, and P. Stott, 2007: A multimodel update on the detection and attribution of global surface warming. Journal of climate, 20 (3), 517{530.

Stott, P. et al., 2006: Observational constraints on past attributable warming and predictions of future global warming. Journal of climate, 19, 3055{3069.

Tett, S. F., P. A. Stott, M. R. Allen, W. J. Ingram, and J. F. Mitchell, 1999: Causes of twentieth-century temperature change near the earth's surface. Nature, 399 (6736), 569{572.

Vyushin, D. and P. Kushner, 2009: Power-law and long-memory characteristics of the atmospheric general circulation. Journal of Climate, 22 (11), 2890{2904.

Vyushin, D. and P. P.J. Kushner, 2012: Modelling and understanding persistence of natural climate variability, submitted.

Wunsch, C., 2003: The spectral description of climate change including the 100 ky energy.

List of Tables

	AR(1) 1850-2005	AR(1) 1850-2012	FD 1850-2005	FD 1850-2012
VOL	0.46	0.48	0.51	0.53
SOL	2.26	2.03	1.14	0.99
GHG	0.94	0.71	0.91	0.66
SUL	2.47	1.44	2.04	0.93
VOL	0.54	0.52	0.55	0.53
SOL	0.98	1.24	0.58	0.83
ANT	0.76	0.71	0.81	0.73

Table 1. Scaling factors obtained from the linear regression when using HADCRUT4 observations for two time periods (1850 to 2005 and to 2012), and the forced temperature responses to VOL,SOL,GHG and SUL forcings , or to VOL, SOL and ANT forcings.

CCMA-CGCM3
CCCMA-CGCM3-1-T63
CNRM-CM3
CSIRO-MK3-0
GFDL-CM2-0
GFDL-CM2-1
GISS-AOM
GISS-AOM
GISS-Model-E-H
GISS-Model-E-R
IAP-FGOALS1-0-G
IAP-FGOALS1-0-G
IAP-FGOALS1-0-G
INMCM3-0
IPSL-CM4
MIROC3-2-HiRes
MIUB-ECHO-G
MPI-ECHAM5
MRI-CGCM2-3
NCAR-CCSM3
NCAR-PCM1
UKMO-HadCM3

Table 2. CMIP-3 General circulation models used partly on the 4th IPCC Assessment report. The order on the table is the same as the numbering in previous gures.

Fig. 1. The 95% con dence intervals of the scaling factors $_i$ derived from the multiregression of observed temperature changes onto the BDM estimates of the forced responses. The internal variability is represented by an AR(1) model (grey line) or an FD model (black line) for the period 1850 2005

Fig.

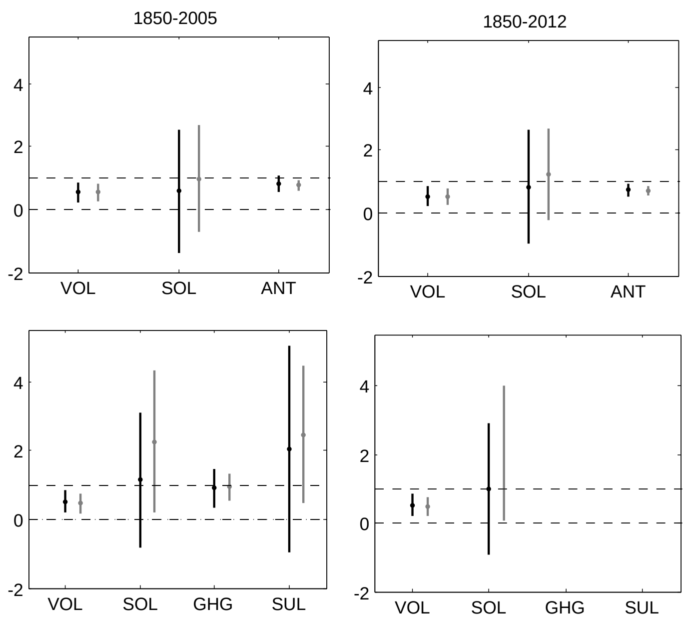

Fig. 3. The 95% con dence intervals of the scaling factors $_i$ derived from the multiregression of observed temperature changes onto the BDM estimates of the forced responses to the three signals VOL, SOL and ANT (top panels) and VOL, SOL, GHG and SUL (bottom panels). The internal variability is represented by an AR(1) model (grey line) or an FD model (black line) for the period 1850 2005 (left hand side) and the period 1850 2012 (right hand side), using HadCRUT4

Fig. 4. Spectra from the individual GCM control simulations (gray), and the spectra of the residuals of the linear t to T_{obs}: T_{obs} $\hat{T}$, when the internal variability is modeled as an AR(1) (thick grey line) and an FD (black line) process. We use a logarithmic scale in the horizontal axis (period) and the vertical axis (spectral density).

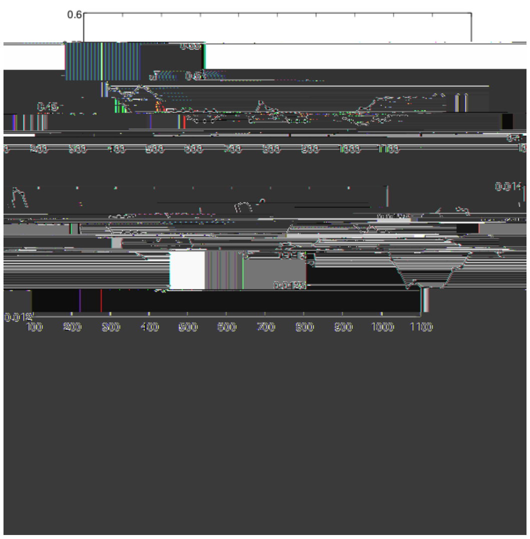

Fig. 5. AR(1) results of estimating a_1 (upper panel) and a_0^2 (lower panel) as a function of the length of the control segment sampled from the 1000 years long HadCM3 control run.

Fig. 6. FD results of estimating (upper panel) and $_e$ (lower panel) as a function of the length of the control segment sampled from the 1000 years long HadCM3 control run.

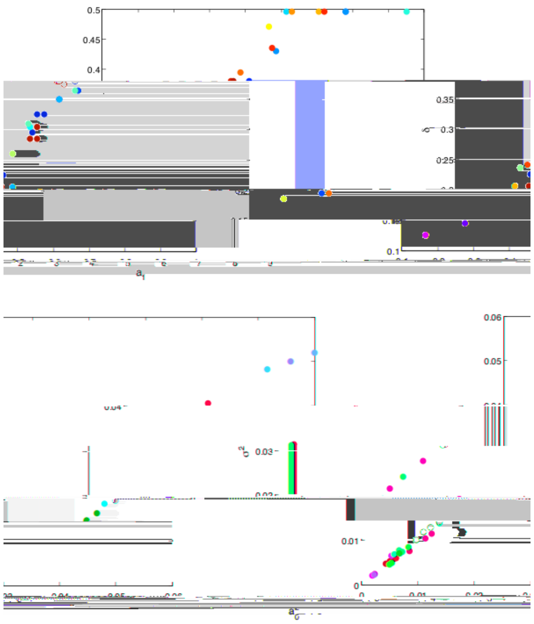

Fig. 7. Upper panel: correlation between the memory parameter of both stochastic models, values (vertical axis) versus a_1 values (horizontal axis) obtained from the CMIP3 control segments considered in our analysis. Lower panel: same for the white noise parameter of both stochastic models, $_e$ (vertical axis) versus a_0^2 (horizontal axis). Each color corresponds to a di erent GCM.